

# Generative Adversarial Networks for Data Generation in Structural Health Monitoring

Furkan Luleci<sup>1</sup>; F. Necati Catbas<sup>1\*</sup>, Ph.D., P.E.; Onur Avci<sup>2</sup>, Ph.D., P.E.

<sup>1</sup>Department of Civil, Environmental, and Construction Engineering, University of Central Florida, Orlando, FL, 32816, USA

<sup>2</sup>Department of Civil, Construction, and Environmental Engineering, Iowa State University, Ames, IA, 50011, USA

**Abstract:** Structural Health Monitoring (SHM) have been continuously benefiting from the advancements in the field of data science. Various types of Artificial Intelligence (AI) methods have been utilized for the assessment and evaluation of civil structures. In AI, Machine Learning (ML) and Deep Learning (DL) algorithms require plenty of datasets to train; particularly, the more data DL models are trained with, the better output it yields. Yet, in SHM applications, collecting data from civil structures through sensors is expensive and obtaining useful data (damage associated data) is challenging. In this paper, 1-D Wasserstein loss Deep Convolutional Generative Adversarial Networks using Gradient Penalty (1-D WDCGAN-GP) is utilized to generate damage associated vibration datasets that are similar to the input. For the purpose of vibration-based damage diagnostics, a 1-D Deep Convolutional Neural Network (1-D DCNN) is built, trained, and tested on both real and generated datasets. The classification results from the 1-D DCNN on both datasets resulted to be very similar to each other. The presented work in this paper shows that for the cases of insufficient data in DL or ML-based damage diagnostics, 1-D WDCGAN-GP can successfully generate data for the model to be trained on.

**Keywords:** 1-D Generative Adversarial Networks (GAN), Deep Convolutional Generative Adversarial Networks (DCGAN), Wasserstein Generative Adversarial Networks with Gradient Penalty (WGAN-GP), 1-D Convolutional Neural Networks (CNN), Structural Health Monitoring (SHM), Structural Damage Diagnostics, Structural Damage Detection

\*Email: [catbas@ucf.edu](mailto:catbas@ucf.edu)

## 1. Introduction

During the life cycle of civil structures, different types of damages can shorten the remaining useful life of the structures. This is particularly important in today's world, where the catastrophic events are in increase, and they are projected to be frequent in the future. Additionally, most civil structures that were built decades ago have already started losing their functionality and capacity. This is especially true for the US where recent studies show the substandard conditions of existing civil structures. Therefore, it is very essential to diagnose the structural damages and subsequently prognose the remaining useful life and based on that implement an effectual health management plan to improve the life cycle of the structure. Hence, with correct maintenance action items derived from health management plan, structural lifetime can be extended, costly structural failures can be avoided, and more importantly, human lives can be saved.

## 1.1. Brief Review on Structural Damage Diagnostics

In the field of Structural Health Monitoring (SHM), the common practice to assess an existing civil structure is to collect operational data using sensors such as accelerometers, potentiometers, strain gauges, fiber optic sensors or load cells. Then damage identification is performed by relating the monitoring data to the structural properties like stiffness, mass, and damping or the changes in the raw data due to induction by structural defects such as crack (fatigue), delamination, spalling, corrosion, bolt-loosening etc. In vibration-based applications, acceleration data is predominantly used since it has advantages such as easy to use and to process the data (Catbas and Aktan, 2002; Catbas et al., 2006; Das et al., 2016).

Vibration-based structural damage diagnostics can be executed in two ways: (1) Local methods where Non Destructive Testing (NDT) and some camera sensing techniques (IR, DIC, RGB etc.) are involved, (2) Vibration based (Global) methods where the collected vibration data is analyzed parametrically (using physical model like FEA software or non-physical model like system identification algorithms to estimate the structure's physical parameters) or nonparametrically (using statistical approaches on the raw vibration data to find the features and then classify or detect the anomalies in it) (Catbas et al., 2016; Avci et al., 2021). Also, using advanced Computer Vision techniques, SHM can be conducted at local and global levels, then damage diagnostics can be performed (Dong et al., 2021).

With the goal of diagnosing structural damages in the civil structures, several studies are presented in the SHM field. In a study by Gul et al. (2008), the authors showed that the boundary conditions of the structure can be indicated by using a deflection profile on a laboratory grid structure. Yin et al. (2009) detected and quantified damage using modal properties extracted with Natural eXcitation Technique (NeXT) and Eigenvalue Realization Algorithm (ERA) from the ambient response of transmission towers. In another study by Krishnan Nair & Kiremidjian (2007), the authors used Auto-Regressive Moving Average (ARMA) to extract and Gaussian Mixture Model (GMM) to classify the features from the collected vibration data and by using Mahalanobis distance, the damage features are identified between damaged and undamaged datasets. Gul & Catbas (2011) used Auto Regressive eXogenous output (ARX) method for time series modelling and extracting the features from the vibration data. They were able to do level-1 (detection) and level-2 (localization) damage diagnostics by using the ARX and clustering the outputs for damaged and undamaged cases for each accelerometer on a grid structure. More recently, Silva et al. (2016) proposed a study where Genetic Algorithm (GA) based clustering is used based on decision boundary analysis (GADBA) to detect structural damages as outliers in the vibration dataset. The above-mentioned studies are parametrically and nonparametrically conducted vibration-based structural damage diagnostic works. One of the common details in those studies is that the amount of collected data is not influential on the success of the proposed algorithms unlike the Machine Learning (ML) and Deep Learning (DL) algorithms where they require plenty of data input – particularly DL algorithms yield exceptionally well results on as much data as possible (Alom et al., 2019).

With the emergence of ML and DL algorithms, they have been used in SHM due to their high performance on feature extraction, classification, regression, and clustering techniques. Several ML methods including parametric and nonparametric vibration-based damage diagnostic studies are introduced. The Artificial Neural Network (ANN) is observed to be the most used algorithm

in ensemble or integrated with different algorithms, and followingly Support Vector Machine (SVM). Some of them are (González et al., 2008; Jungwee Lee et al., 2007; Cury et al., 2012; Jong Jae Lee et al., 2005; Gul et al., 2014; Santos et al., 2016; Bandara et al., 2014; Ghiasi et al., 2016; Abdeljaber et al., 2016). Furthermore, it is important note that apart from parametric-based methods where they rely on system identification techniques to extract the structural parameters, using a ML model for nonparametric-based damage diagnostic requires the usage of feature extraction from the raw data (Catbas and Malekzadeh, 2016) such as Principal Component Analysis (PCA) or Autoregressive (AR). Thus, this causes computational complexity and time along with other limitations (Avci et al., 2021). The DL algorithms can learn to extract useful features from the raw data and train on them to make accurate predictions. In short, with a correctly built model and proper training, DL models can show superior performance over ML models. In the civil SHM field, there are few studies including vibration based unsupervised DL - mostly Autoencoders (Pathirage et al., 2018; Shang et al., 2021; Rastin et al., 2021) and few supervised DL – mostly Convolutional Neural Networks (Abdeljaber et al., 2017; Yu et al., 2019; Avci et al., 2017; Abdeljaber et al., 2018; Eren, 2017).

## **1.2. Motivation and Objective**

In civil SHM, data collection is a challenging and expensive task such as getting permission from authorities to install expensive and laborious SHM systems, setting up communication networks between sensors and data acquisition systems, requesting traffic closures, and having skilled experts on the field. Additionally, obtaining useful data containing damage associated features is not always very easy. This is partially one of the outcomes of previously mentioned SHM challenges. Considering that only a few civil structures have permanent SHM systems in the world, it is also difficult to know about damage state of the remaining structures. As such, data scarcity is a challenge in civil SHM. One solution for that is oversampling the dataset by increasing the copy of the existing dataset. However, this solution does not teach the AI models to learn the variation in the damage-associated data but teach only the provided one to the model and may lead overfitting. Building an FEA model and analyze the structure under similar damage scenarios then producing displacement, stress, or acceleration data is another solution to tackle the data scarcity challenge. Yet, this methodology can be inaccurate and possibly unreliable compared to real data from particularly complex structures. In addition, it is very unlikely that observed damages can be reflected correctly in a model along with accumulated numerical FEA errors (Gardner & Barthorpe, 2019).

As the focus shifted towards ML and DL models for the damage diagnostics of civil structures, aforementioned data scarcity problem hinders the usage of these algorithms since they require large datasets. The study presented in this paper employs Generative Adversarial Networks (GAN) to generate useful data to be further used by a Deep Convolutional Neural Network (DCNN) model to perform nonparametric damage diagnostics on the existing data of a steel laboratory structure. Specifically, the presented study investigates vibration-based damage detection with scarce data, where GANs can generate data for the ML or DL model to be trained on and then perform damage identification. The proposed methodology in this paper will enable SHM procedures to be performed when the data is scarce.

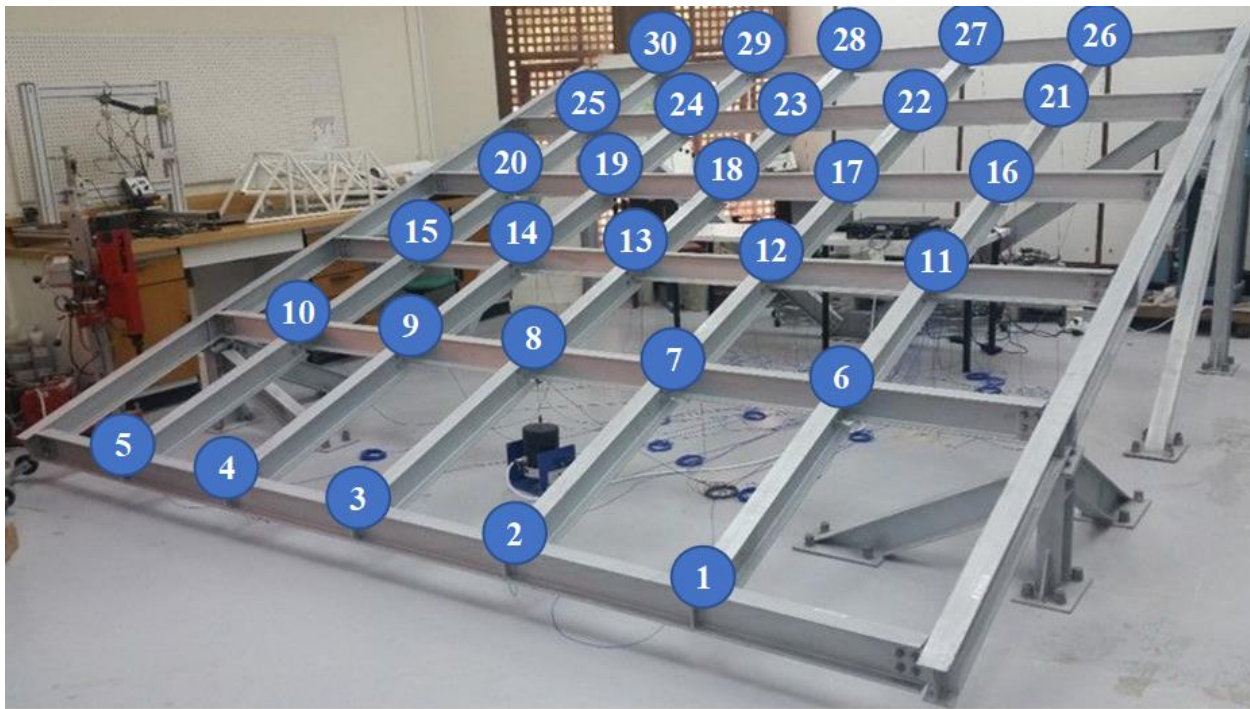
### 1.3. Background on the GAN

Goodfellow et al. (2014) introduced a novel framework containing two separate networks: a generative model that captures the given random data distribution and tries to maximize the likeliness of the output it produces very similar to the training input, and a discriminative model that tries to maximize the possibility of the data it receives from the generator is fake and from the training input is real. In that manner, it is considered as a two-player game where each side is trying to deceive each other. The methodology is used successfully on image-based applications. Yet, among the other DL networks, training GANs might be the most challenging one. For instance, they are very hard to converge due to finding a unique solution to Nash equilibrium where the optimization process is looking to find a balance between two sides instead of a minimum. GANs often experiences large oscillation during the training which makes it harder to reach a convergence. Another issue is the mode collapse where the generator part produces same outputs due to learning a feature in the data that can be used to trick the discriminator easily. Also, intuitively, GANs suffer from the discriminator being powerful over the generator which causes the generator training to fail due to vanishing gradients, thus, the discriminator does not provide sufficient information for the generator to learn (Ian Goodfellow, 2016; Salimans et al., 2016). There are several “hacks” introduced to alleviate these drawbacks in the DL community and some of them are used in this study as well as discussed in the following sections. Radford et al. (2015) proposed using the DCNN in GANs after their adoption in computer vision applications. In their study, they noticed that in the training process, DCNN helped the GAN to learn significantly. Yet, Arjovsky et al. (2017) introduced a GAN that uses Wasserstein distance as a loss function (WGAN) which improves the training of GAN. In their network, instead of using a discriminator which estimates the probability of the generated images as being real or fake, they used a critic which scores the output’s realness or fakeness of a given image. Fundamentally, WGAN seeks a minimization of the distance between the generated and the training data distribution. WGAN showed huge benefit to training the GAN such as more stable, less sensitive to the parameters and model architecture, loss functions are more meaningful as they directly relate to the quality of generated images. Gulrajani et al. (2017) proposed using a penalization of the gradient during the training of the critic due to using weight clipping on the critic which enforces the Lipschitz constraint and therefore lowers the learning capacity of the model. They named the model Wasserstein Generative Adversarial Networks with Gradient Penalty (WGAN-GP). The authors showed that the proposed method performed better than WGAN and provided more stable training.

GANs are mostly used in computer vision field which process on 2-D data. Also, there are some studies in different disciplines attempted to use GANs for 1-D data generation and reconstruction for different purposes (Truong et al., 2019; Kuo et al., 2020; Luo et al., 2020; Wulan et al., 2020; Tiantong Wang et al., 2021; Sabir et al., 2021). In the SHM field of non-civil structures, some studies of GAN based 1-D data generation, reconstruction, and then training an ML classifier are introduced (Shao et al., 2019; Guo et al., 2020; Gao et al., 2019; Xuewen Zhang et al., 2021). In the SHM field of civil structures, few studies are introduced related to using GAN for 1-D data reconstruction, (C. Zhang et al., 2018; Fan et al., 2021; Jiang et al., 2021). However, no study investigated the usage of WGAN and WGAN-GP extensively to address the insufficient data problem for civil structures and test the generated output on a DCNN model for vibration-based damage diagnostic.

## 2. Methodology

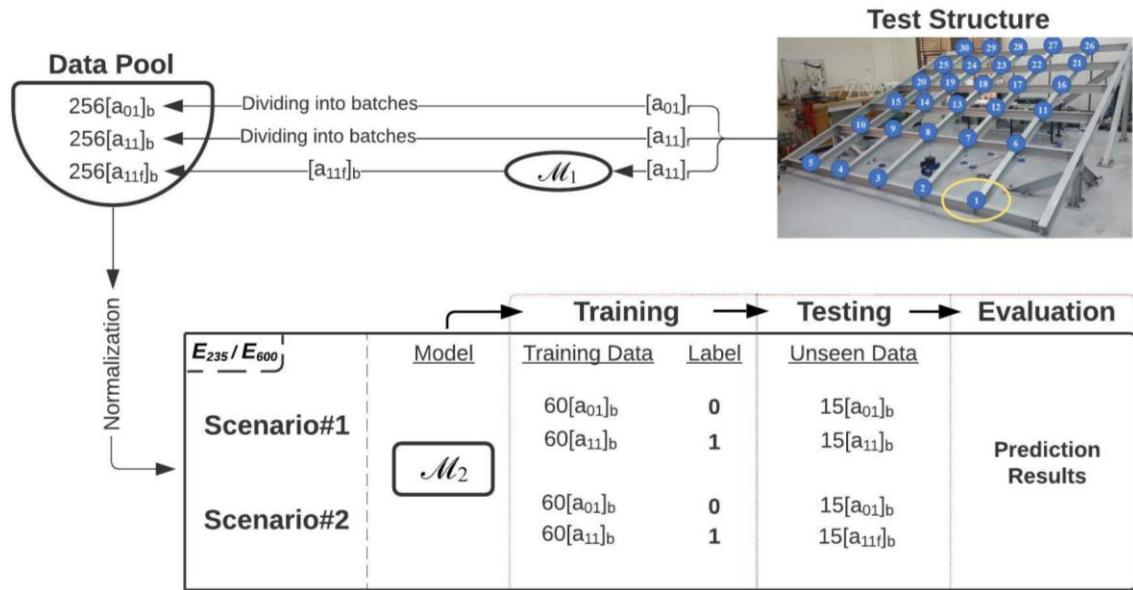
The authors of this study used WGAN-GP that is built on a DCNN which is named WDCGAN-GP. Since the used data in this study is 1-D, all the convolution operations are executed 1-D both for WDCGAN-GP and DCNN. Thus, in short, 1-D WDCGAN-GP is utilized to generate a synthetic dataset and 1-D DCNN to perform nonparametric damage identification. For simplicity, in the rest of the paper 1-D WDCGAN-GP and 1-D DCNN is referred to as  $\mathcal{M}_1$  and  $\mathcal{M}_2$ , respectively. The workflow followed in this study can be summarized in this order: (1) Data preprocessing for  $\mathcal{M}_1$ , (2) Building the  $\mathcal{M}_1$ , (3) Training and fine-tuning the  $\mathcal{M}_1$ , (4) Evaluation and interpretation of results from the  $\mathcal{M}_1$ , (5) Data preprocessing for the  $\mathcal{M}_2$ , (6) Building the  $\mathcal{M}_2$ , (7) Training and fine-tuning the  $\mathcal{M}_2$ , (8) Testing the  $\mathcal{M}_2$ , (9) Evaluation and interpretation of the results from the  $\mathcal{M}_2$ . In the following paragraphs, the dataset, technical notations, and workflow are explained.



**Fig. 1.** Steel Frame Grand Simulator Structure (Abdeljaber et al., 2017)

The vibration dataset is obtained from the study conducted by Abdeljaber et al. (2017) on a steel laboratory frame (Fig. 1) where total of 30 accelerometers installed at each 30 joints and a modal shaker excitation is applied on the structure. Respectively, 30 different damage and 1 undamaged scenarios are created at each 30 joints separately by loosening the connection bolts of the joints between filler beams and girders. Then, they collected 256 seconds of vibration data at a sampling rate of 1024 Hz with a total sample of 262,144. The tensor notation used in this paper,  $n[a_{xyf}]_s$  where  $x$  represents the condition such as 0 means data is collected in an undamaged scenario, 1 is damaged scenario,  $y$  represents the joint number where the vibration data is collected at,  $f$  refers to “fake” if it is generated by the  $\mathcal{M}_1$ . The  $s$  refers to number of sample that a tensor contains, and  $n$  refers to “number” of tensors, if there is no number then it is 1 tensor. This study worked on only two different size of sample. To represent the size of tensors in a simple way, 262144 and 1024

samples are denoted as  $r$  and  $b$  respectively where  $r$  refers to “raw” and  $b$  refers to “batch”. The generated data from the  $\mathcal{M}_1$  is 1024 sample size; it is also the used batch size in the model. For DCNN to use the raw and generated tensors together, raw tensors are also divided into 1024 size of batches randomly (note that the output tensors from the GAN are also generated randomly since the input,  $[a_{11}]_r$ , is batch sampled in shuffle during the training). A similar method is also successfully implemented in a study by Abdeljaber et al. (2017) where they divided the raw vibration signal into frames and shuffled it randomly. Besides, since the purpose of this study is to demonstrate that GANs can tackle the data scarcity problem for nonparametric damage diagnostics for civil structures, the sequence or the parameters of the signal tensors are irrelevant. The PC used in this study has following specs: 16 GB RAM DD4 2933 MHz and NVIDIA GeForce RTX 3070 8GB GDDR6 graphic card.



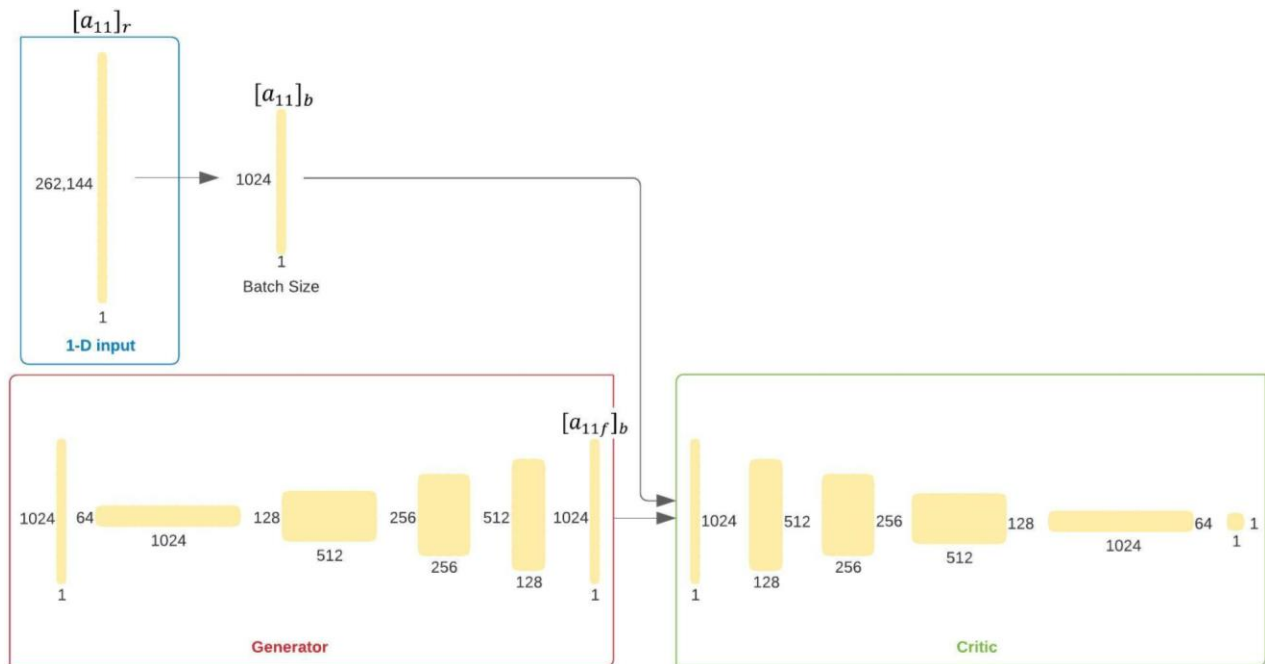
**Fig. 2.** The Workflow

Fig. 2 represents the workflow of this study where tensors  $[a_{01}]_r$  and  $[a_{11}]_r$  are divided into 256 batches each. Then,  $[a_{01}]_b$  and  $[a_{11}]_b$  are extracted to the data pool. The tensor  $[a_{11}]_b$  inputted in the  $\mathcal{M}_1$  model to generate synthetic data of  $256[a_{11f}]_b$ . Followingly, these tensors are used in  $\mathcal{M}_2$  for two different scenarios. The test dataset is taken as 25% of the training data in each scenario. In Scenario#1, normal conditions are assumed in which the undamaged and damage datasets are real tensors. To represent that,  $60[a_{01}]_b$  and  $60[a_{11}]_b$  are used in training and  $15[a_{01}]_b$  and  $15[a_{11}]_b$  are used in testing dataset. In Scenario#2, for training the model, real undamaged and damaged tensors are used but for testing, generated damaged along with real undamaged tensors are used. To represent that,  $60[a_{01}]_b$  and  $60[a_{11}]_b$  are used in training and  $15[a_{01}]_b$  and  $15[a_{11f}]_b$  are used in testing. In The Scenario#1 is created to form a reference line for comparability purposes with the other scenarios. Scenario#2 aims to demonstrate the performance of  $\mathcal{M}_1$  as to how accurate can  $\mathcal{M}_2$  be trained on a real data and make correct predictions on a generated and real data. In other words, it is to evaluate to what extent  $\mathcal{M}_2$ , which was trained using real data, can make correct predictions on the fake damaged and real undamaged data. Furthermore, the workflow shown in Fig. 2 is repeated on the same  $\mathcal{M}_1$  configuration twice for

validation and to investigate the effect of more training on the outputs as well as on the decision by  $\mathcal{M}_2$ . Hence, the case where  $\mathcal{M}_1$  is trained with less epochs (iterations) is denoted as  $E_{235}$  and the one with more epochs as  $E_{600}$ . Next sections explain the  $\mathcal{M}_1$  and  $\mathcal{M}_2$  workflow in detail.

## 2.1. $\mathcal{M}_1$ - Data Preprocessing

The common practice for DL models before training is to make datasets in the same scale for the model to learn and predict more efficiently. Additionally, during the front and back propagation through the network where the dot product of weights is calculated, normalization helps the model to yield more accurate results and less computation time. Thus, normalization is not needed unless the vibration data has spikes. Otherwise, the spikes would have huge impact on the weight propagation which can lower the model quality in training. Also, the  $\mathcal{M}_1$  model consists of batch and instance normalization layers that normalize the data batches during the training. Considering that the dataset does not contain large spikes, the model is tried with both normalized and raw training input and it is observed that results are not distinctly different. In fact, it is believed that the model captures the spatial-temporal features better when it receives the raw vibration dataset. Hence, normalization is not implemented before the training.



**Fig. 3.** 1-D WDCGAN-GP ( $\mathcal{M}_1$ ) Architecture

## 2.2. $\mathcal{M}_1$ - Architecture

After several trials of different model architectures, the one used in this study is shown in Fig. 3. First, the generator receives the dimensional noise tensor ( $z$ ) and passes it through five 1-D transpose convolutions which the first layer is  $filter = 64, stride = 2, padding = 0$ , then the rest are  $filter = 4, stride = 2, padding = 1$ . Batch Normalization and then ReLU is used for after every convolution layer except the last one. After the last convolution layer, Tanh function is used. Consequently  $[a_{11f}]_b$  is created. Following this, the training input  $[a_{11}]_b$  and the generated



tensor  $[a_{11f}]_b$  are passed to the critic (which is called the “discriminator” in GAN but in WGAN, it is “critic”) to be evaluated as to how real or fake each tensor is. The critic takes the tensor and passes it through five 1-D convolutions which the first four layers are  $filter = 4, stride = 2, padding = 1$  and the last layer is  $filter = 64, stride = 2, padding = 0$ . After the first convolution layer, Leaky ReLU and then Dropout is used. Then, after every second, third, and fourth convolution layers, Instance Normalization and then Leaky ReLU is used.

### 2.3. $\mathcal{M}_1$ - Training and Fine Tuning

As mentioned, GANs are arguably the most difficult DL models to train among other DL models. Therefore, it requires considerable effort on fine-tuning. Although the model used in this study, 1-D WDCGAN-GP, is one of the most robust GAN models in the literature, few approaches have taken during the fine-tuning after many trials with different hyperparameters. First, using one layer of dropout with 70% in the critic found beneficial in training. Thus, the capacity of the critic reduces and balances the equilibrium between two adversarial networks and avoids the overfitting problem. Next, a decaying random Gaussian noise is added to the training input to decrease the learning rate of the critic. The learning rate of  $5 \times 10^{-6}$  for generator and  $2 \times 10^{-5}$  for critic gave the best result. The critic iterations, lambda parameter for the gradient penalty, and batch size are respectively picked as 12, 20, and 1024, respectively. The number of epoch used is 235 (case  $E_{235}$ ) and 600 for (case  $E_{600}$ ). It took 18 hours and 44 hours of training respectively. Lastly, AdamW optimizer is used in both the generator and critic.

### 2.4. $\mathcal{M}_1$ - Evaluation and Interpretation of Results

Evaluation of the GAN models can be categorized as qualitative and quantitative evaluation where the former one is based on visual evaluation and the latter one is based on numerical evaluation. The most used form of evaluation of GANs used in the DL field is visually comparing the output of the generator with the training data, which are mostly images. Yet, this qualitative approach might not be an easy or efficient way for 1-D data as it suffers from some limitations such as limited number of generated output can be viewed by an observer in limited time or observed subjectively by different observers. Also, unlike the other DL models, GANs lack of objective function which makes it difficult to evaluate the performance of the model. That’s why there are several methods to evaluate the performance of the model with no reached consensus in the DL field yet as to which quantitative measure is the most effective. The study from Borji (2018) investigated the evaluation methods of GANs and readers are directed to that reference. Recently, the Fréchet Inception Distance (FID) score is introduced (Heusel et al., 2017) and have become the most used quantitative evaluation method for GANs as several studies proved its effectiveness against other methods such as Inception Score (IS). The FID score is introduced as an improvement over the IS which lacks capturing the similarity of real input to the produced output. Particularly, the FID has showed very consistent results when compared with qualitative evaluation of the GAN outputs. The FID formula is based on a statistical formulation which is provided in equation 1.

$$FID(x, g) = \|\mu_x - \mu_g\|_2^2 + Tr(C_x + C_g - 2(C_x C_g)^{0.5}) \quad (1)$$

Where  $\mu_x$  and  $\mu_g$  are the means,  $C_x$  and  $C_g$  are the covariance matrices of real and generated signals respectively, and  $Tr$  is the trace of the matrices e.g., the sum of all the diagonal elements in the matrices. Lower the FID score, the more similar the compared datasets. Structural Similarity Index



Measure (SSIM) (Z. Wang et al., 2004) is another quantitative evaluation metric which is mostly used for image quality assessment of two images based on a statistical formulation. For instance, if the images are same, the SSIM is 1 and if they are different, it is 0. A paper by Sabir et al. (2021) conducted a successful study on a signal data where they evaluated the GAN outputs based on the creativity and diversity approaches using SSIM. For example, creativity indicates that generated signals are not the exact ones of the real data and diversity indicates that how the generated datasets look like each other. In their study, they used the threshold of 0.8 for investigating creativity and if the SSIM of two signals is higher than 0.8, it is concluded that signals are duplicate. These measures are important for evaluating the GANs as they are expected to add creativity and diversity to the outputs (Guan et al., 2020). Yet, there is no consensus on what SSIM value is good for creativity and diversity for evaluating GANs. In this study, creativity approach is investigated considering the threshold value of 0.8; also, the diversity approach is explored based on how the SSIM values are close to 1 and 0. While the creativity is explored by using the SSIM of the generated and real tensors and the diversity is explored by using the SSIM of the generated tensors within the entire generated dataset. The SSIM formula is given below in equation 2.

$$\text{SSIM}(x, g) = \frac{(2\mu_x\mu_g+c_1)(2\sigma_{xg}+c_2)}{(\mu_x^2+\mu_g^2+c_1)(\sigma_x^2+\sigma_g^2+c_2)} \quad (2)$$

Where  $\mu_x$  and  $\mu_g$  are the means,  $\sigma_x$  and  $\sigma_g$  are the standard deviations, and  $\sigma_{xg}$  is the covariance of real data ( $x$ ) and generated data ( $g$ ) respectively. The  $c_1$  and  $c_2$  are the constants which are multiplication of  $k_1$  and  $L$ , and  $k_2$  and  $L$ , respectively to stabilize the division with weak denominator where  $L$  is the dynamic range of the signal and  $k_1$  and  $k_2$  are the constants which are picked in this study as 0.01 and 0.03.

During the training of both  $E_{235}$  and  $E_{600}$ , the critic and generator losses and FID scores are plotted to monitor the learning process of the model. The critic losses are converging near zero. The generator losses are first increasing as the one that is superior, the critic, rejecting outputs of the generator since critic has more knowledge on the real data domain. However, after the generator starts learning the gradients and produce more real-looking datasets, it is seen to be returning to its first loss value which is expected for WGAN-GPs (Fig. 4-Generator Loss tagged plots). The FID calculations are made between the batches,  $[a_{11f}]_b$  and  $[a_{11}]_b$  and they seem to be reducing to zero for both cases, which means they are getting similar to each other (Fig. 4-FID tagged plots).

To ensure that  $[a_{11f}]_b$  is not only getting similar to  $[a_{11}]_b$  but also to  $[a_{11}]_r$ , which is the input of  $\mathcal{M}_1$ , the FID between  $[a_{11f}]_b$  and  $[a_{11}]_r$  is computed. The training results show that the FID scores between  $[a_{11f}]_b$  and  $[a_{11}]_b$ , and the FID scores between  $[a_{11f}]_b$  and  $[a_{11}]_r$  are following similar path during the training (Fig. 4-FID tagged plots). This also reveals that the sampled batches,  $[a_{11}]_b$ , from the real input,  $[a_{11}]_r$ , have repetitive features in a particular sample length in 262,144 samples. Thus, it validates the study to continue using the 1-second tensors such as  $[a_{11f}]_b$ ,  $[a_{11}]_b$ , and  $[a_{01}]_b$ . Since the aim is nonparametric damage diagnostics, it is not based on any parameters but on raw data, hence the order of the samples in datasets is irrelevant. Therefore, the method of sampling with 1-second batches in shuffle mode from the original input is used, which helps the training of the model for faster convergence, preventing bias, preventing learning the order of the data etc. Thus, for the rest of the study, only the calculations between batch sampled generated and real data ( $[a_{11f}]_b$  and  $[a_{11}]_b$ ) are considered. Furthermore, during the training, in the  $E_{235}$  case,

the FID score started from 0.0345 and decreased to 0.0021 which means a reduction of around 16 times and in the case  $E_{600}$ , the FID score started from 0.1359 and decreased to 0.000015, a reduction of 9060 times. The large difference in the reduction value shows that the number of training epoch helped the model to learn the dataset thoroughly. For a better understanding of the FID score values, study by Costa et al. (2019) can be informative. Costa et al. compared their GAN model to others on MNIST dataset and the FID score decreased by 6 times during the training. Although the 9060 times decrement can be viewed as success, it can also be an indication of overfitting for the case  $E_{600}$  which will be investigated in the following paragraph.

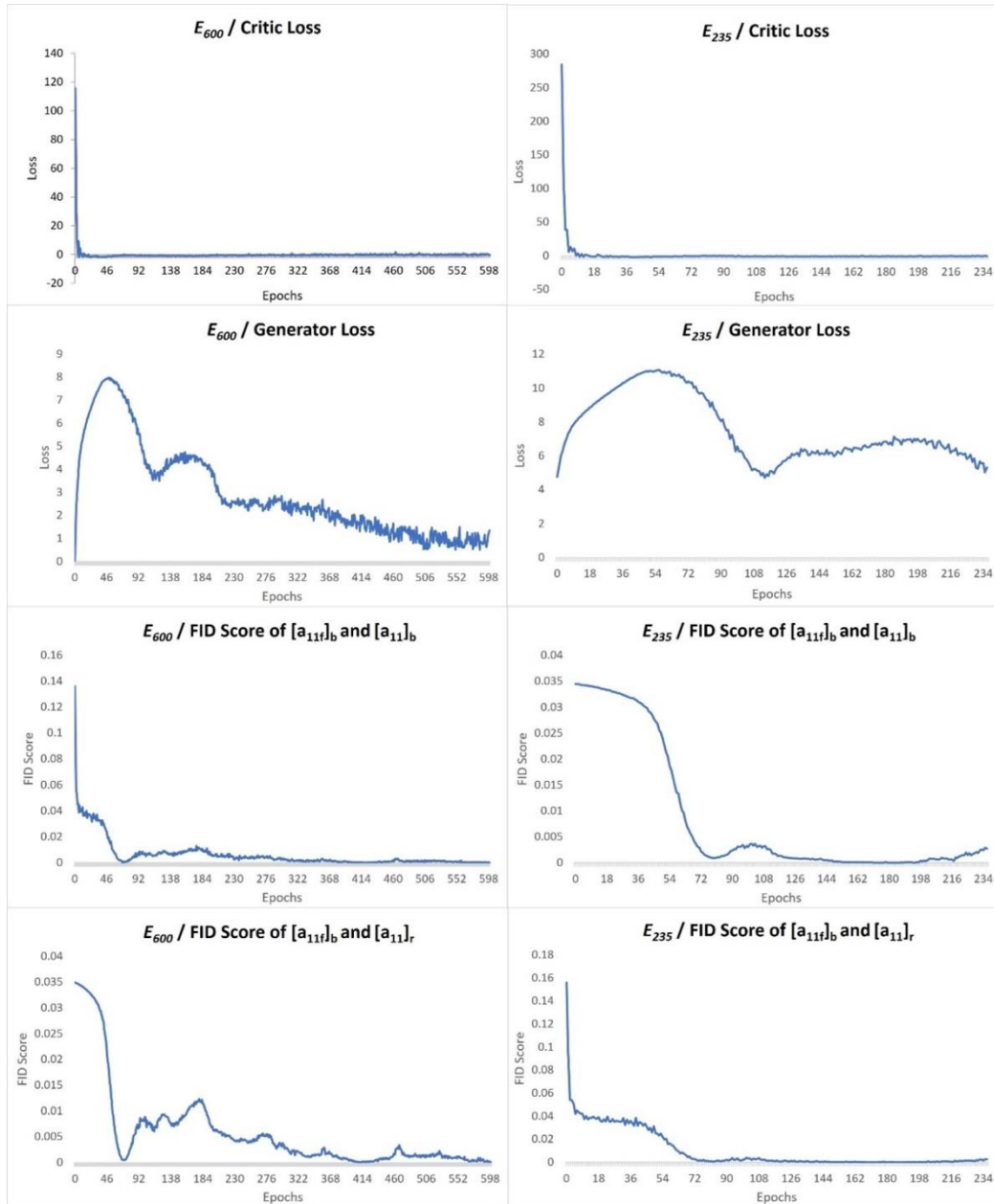


**Fig. 4.** Training plots of GAN for case E235 and E600

Moreover, the trained  $\mathcal{M}_1$  model is used to generate  $256[a_{11f}]_b$  for each  $E_{235}$  and  $E_{600}$  case to extract into the data pool as discussed before. Then the FID scores are computed for the generated between the real tensors. Subsequently, the Probability Density Function (PDF) is plotted to visualize the density differences for each case in Fig. 5. It is seen that the FID scores for the case  $E_{600}$  is cumulated around 0.0007 with lower variance which means that the model learned the dataset in depth and narrowed the features in the synthetic data that looks similar to the original input. For the case  $E_{235}$ , the PDF is cumulated around 0.0025 with higher variance which means that the model’s entropy is larger, in other words more uncertainty involves in the learned dataset and the model needs to be trained more. In summary, the generated outputs in case  $E_{600}$  are very similar to the real data and can be concluded that the model learned training data.

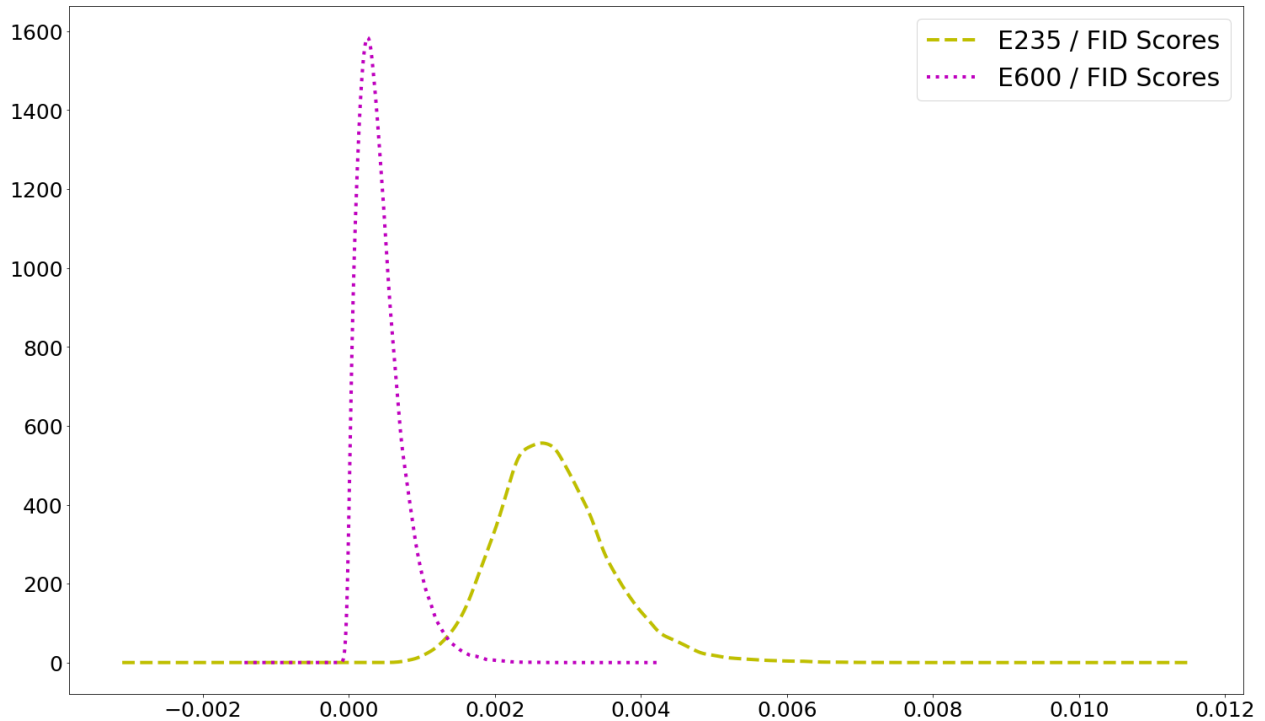


**Fig. 5.** Plot of Probability Density Functions of FID scores for  $E_{235}$  and  $E_{600}$

Next, the creativity and diversity measures are investigated for both cases,  $E_{235}$  and  $E_{600}$ . Firstly, the SSIM between the  $[a_{11f}]_b$  and  $[a_{11}]_b$  is computed and the PDFs of the SSIM results are plotted in Fig.6. The SSIM does not go above 0.8 threshold value which can be concluded that the generated tensors,  $[a_{11f}]_b$ , are not the exact copies of the real tensors,  $[a_{11}]_b$ , thus  $\mathcal{M}_1$  can generate creative outputs. The Fig.6 indicates that in the case  $E_{600}$ , the generated tensors are more similar to the real tensors as the SSIM values are cumulated around 0.3 and this value is 0.23 in the case  $E_{235}$ . This measure also determines the overfitting of the model which is not the case for our model here because no exact copies exist since computed values are significantly lower than the threshold value of 0.8. Secondly, the SSIM within the generated tensors,  $[a_{11f}]_b$ , are computed to investigate the diversity of the generated tensor and found that the tensors in the case  $E_{600}$  are slightly more similar to each other than the one in case  $E_{235}$ . This can be interpreted as since the  $\mathcal{M}_1$  in case  $E_{600}$  is trained more, it learned the data more than the  $\mathcal{M}_1$  in case  $E_{235}$ . From the SSIM results for both cases for creativity and diversity investigation purposes, conclusion can be made that none of the

generated and real tensors are the exact copies of each other nor the generated tensors of each other.

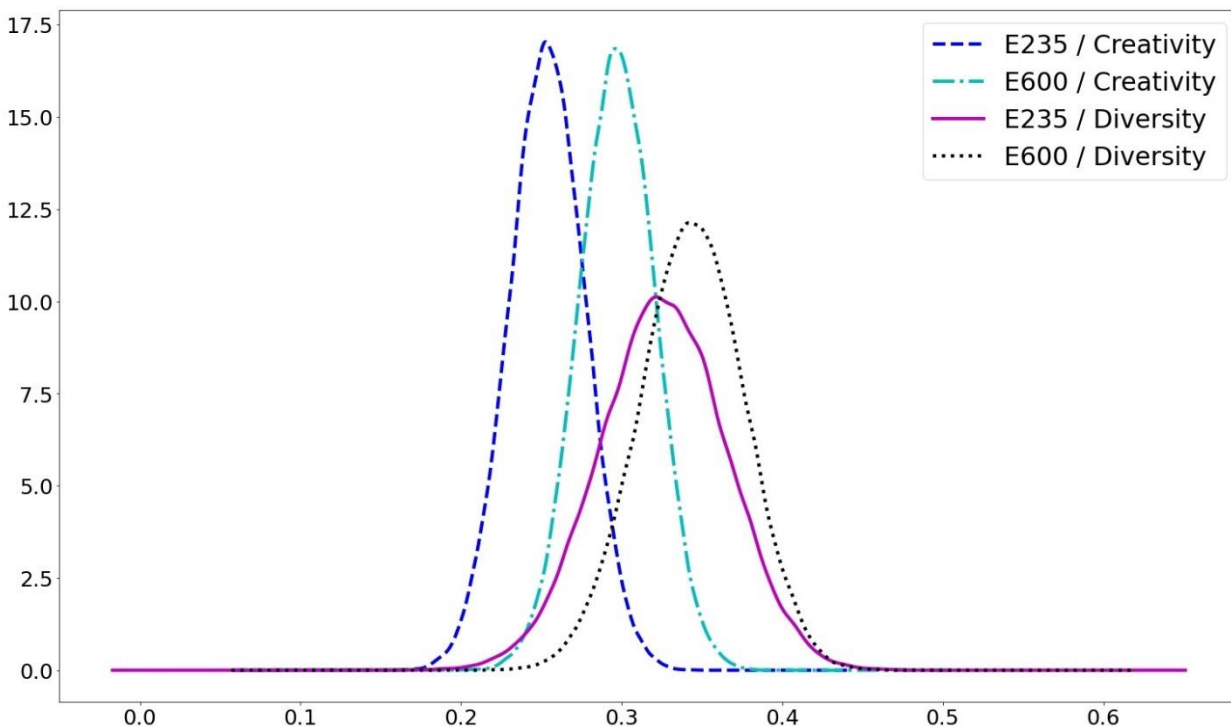


**Fig. 6.** Plot of Probability Density Functions of Creativity and Diversity measures for cases  $E_{235}$  and  $E_{600}$

As a last step of the quantitative evaluation of the results, the box plots are used for both cases,  $E_{235}$  and  $E_{600}$  separately. For that, one with lowest and one with highest FID scores of two different real and generated tensors are box plotted in Fig.7. As the  $\mathcal{M}_1$  is trained more, the variance of the generated dataset gets more closer to the real dataset along with the maximum and minimum values. It can be also observed that the lower the FID score is the more box sizes and whiskers of the generated and real data are getting similar. As a result, the box plots show that the statistical meaning and distributions of the generated and real data pairs are looking very similar, especially in the case  $E_{600}$ .

To conduct a qualitative evaluation, which is the most preferred and effective method for evaluating the image data (yet it suffers from its limitations as previously mentioned), the same vibration tensor pairs that were used in Fig.7 are plotted in Fig. 8 and Fig. 9. Although it is not trivial to judge the similarity between the tensors as doing it on the 2-D image data, there is a good consistency between each tensor pairs.

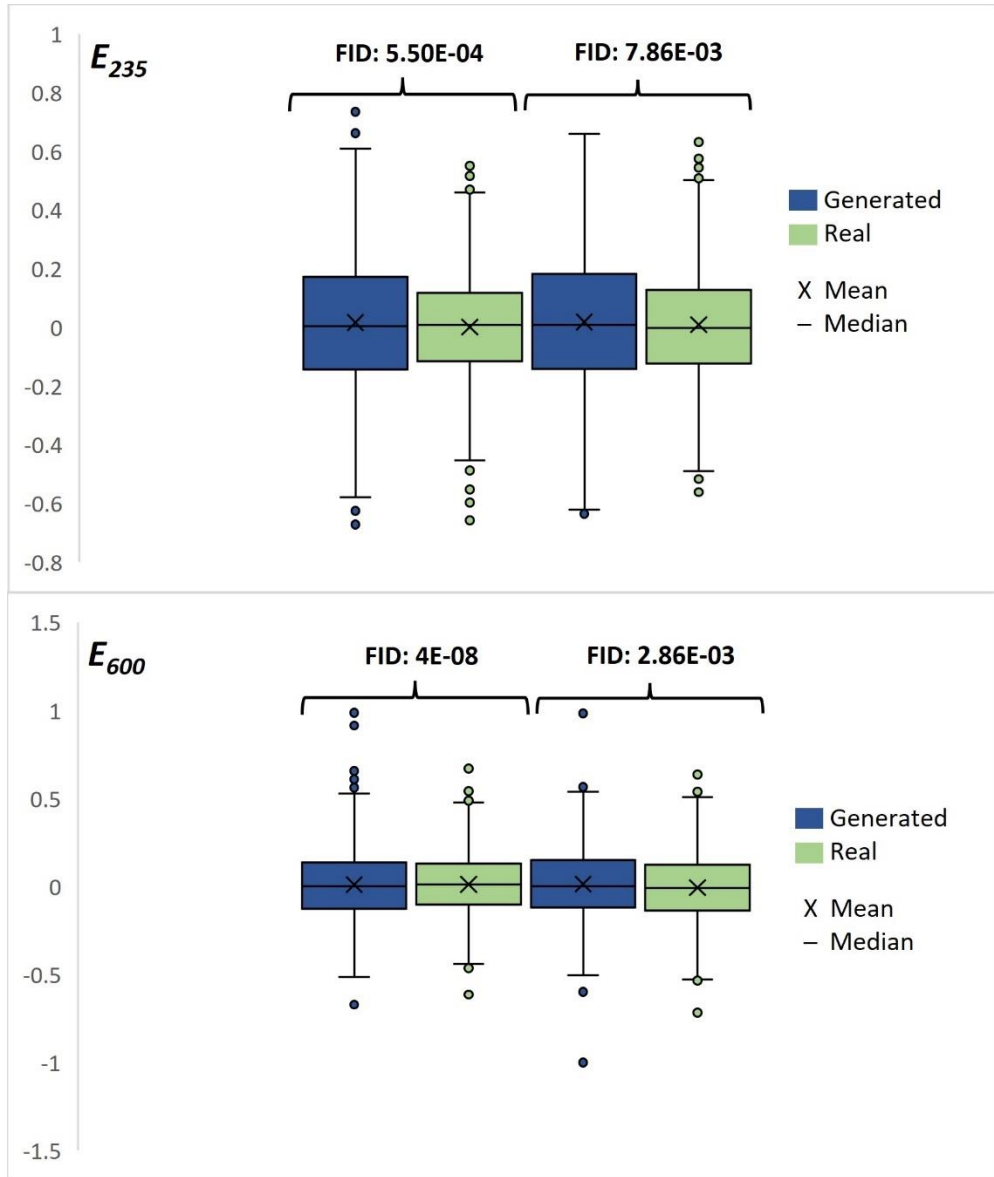


**Fig. 7.** Box plots of the tensors for case  $E_{235}$  and  $E_{600}$  with lowest and highest FID values

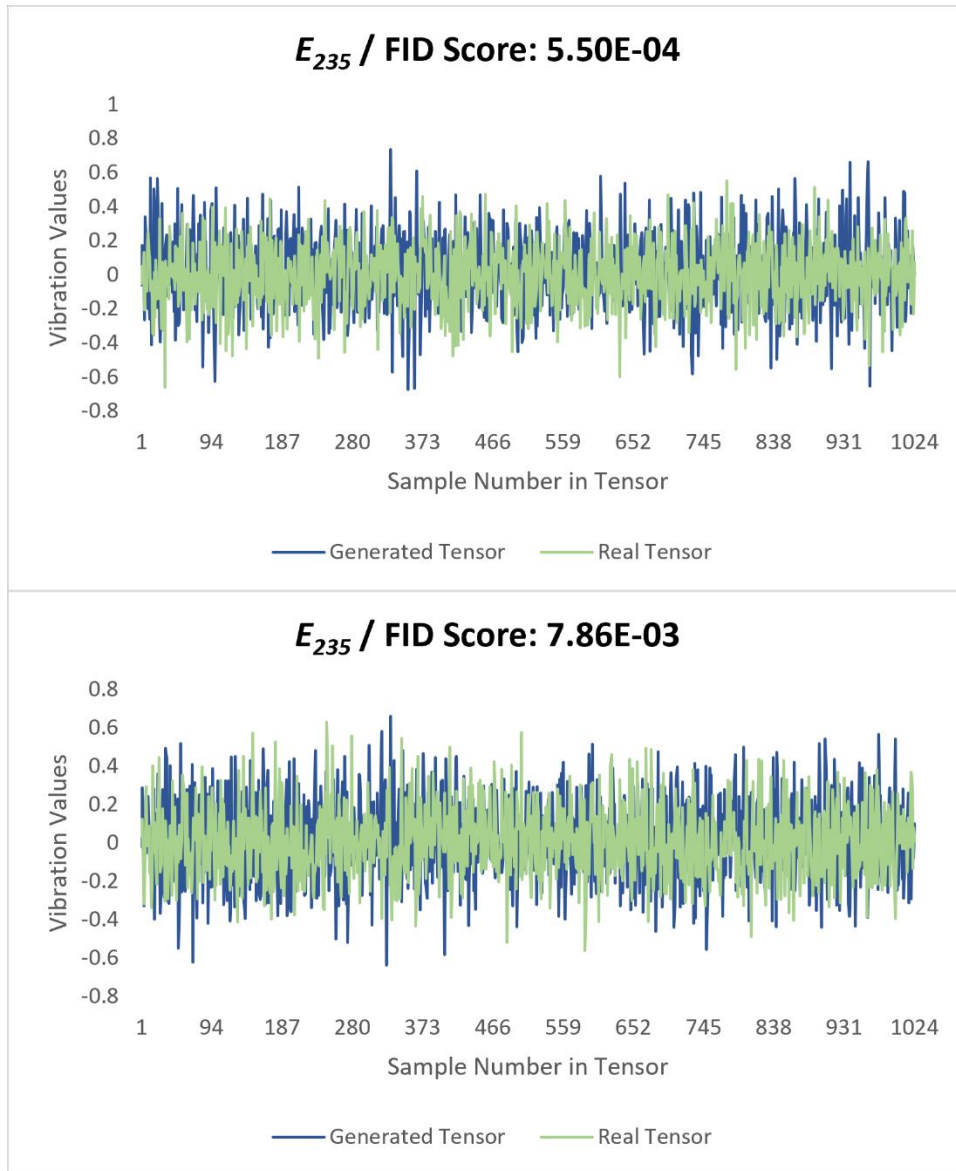


**Fig. 8.** Plotted tensor pairs for case  $E_{235}$  with lowest and highest FID values

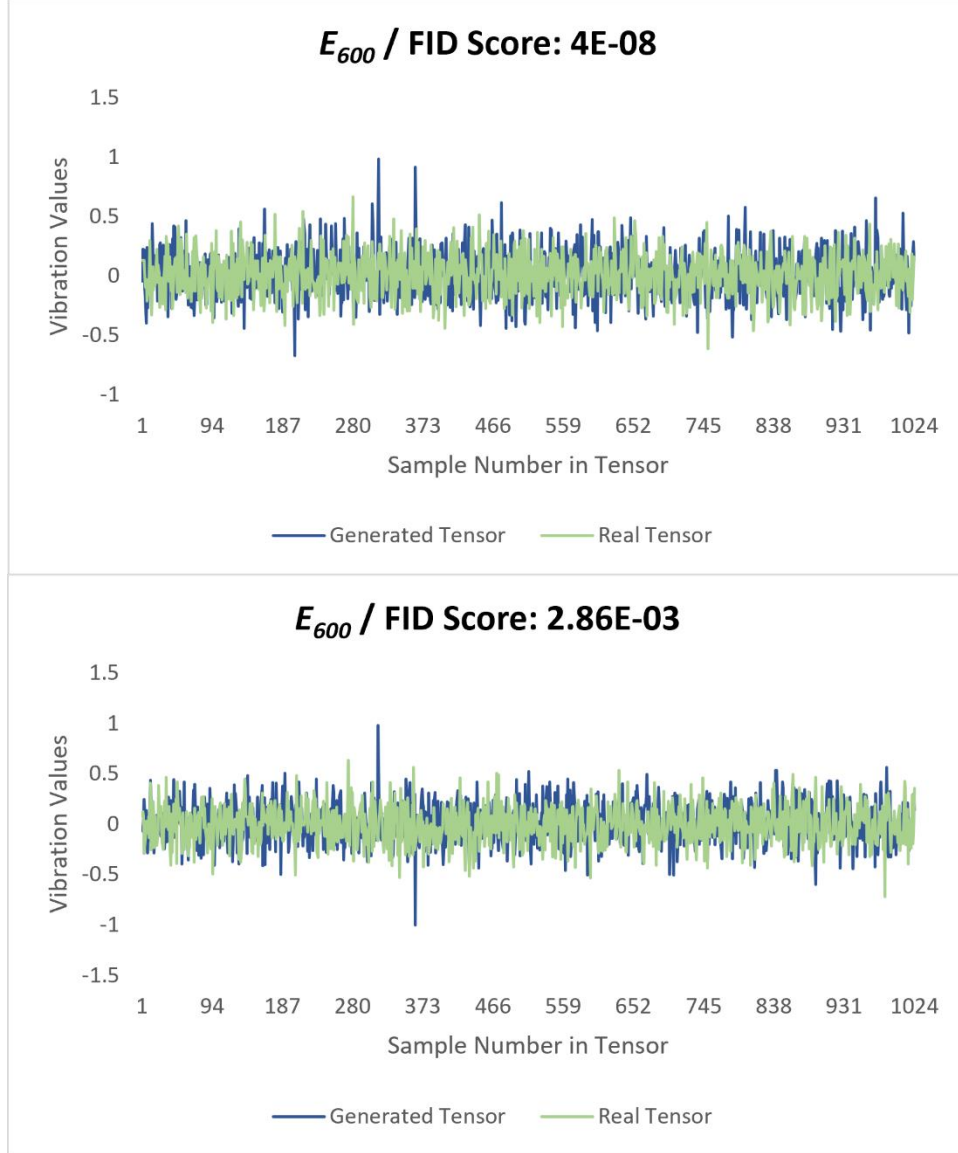


**Fig. 9.** Plotted tensor pairs for case  $E_{600}$  with lowest and highest FID values

## 2.5. $\mathcal{M}_2$ - Data Processing

Unlike the procedure in the  $\mathcal{M}_1$ –Data Processing section, the tensors from the data pool,  $[a_{11}]_b$ ,  $[a_{11f}]_b$ , and  $[a_{01}]_b$  are normalized between -1 and +1 range before feeding into  $\mathcal{M}_2$ . Subsequently, the tensors are randomly extracted without replacing from the data pool as designated order in Fig. 2 for the training of  $\mathcal{M}_2$ .

## 2.6. $\mathcal{M}_2$ - Architecture

The architecture used in  $\mathcal{M}_2$  is the same architecture that is used in  $\mathcal{M}_1$ 's critic network. Additionally, as there was no activation function used at the end of the last layer in critic in the  $\mathcal{M}_1$  process (only realness or fakeness scores were used in critic), sigmoid function is used in the



$\mathcal{M}_2$  phase which results with prediction score in range of 0 to 1 where 0 is labelled as undamaged and 1 as damaged in this work. Lastly, no dropout is used since there is no use of it for the purpose of simple detection procedure.

## 2.7. $\mathcal{M}_2$ – Training and Fine Tuning

Like in the procedure of  $\mathcal{M}_1$ , the parameters are chosen for  $\mathcal{M}_2$  after many trials. For each case  $E_{235}$  and  $E_{600}$  and each Scenario#1 and Scenario#2, the used learning rate, batch size, and number of epoch are  $8 \times 10^{-4}$ , 30, and 300, respectively. AdamW and Binary Cross Entropy is used as an optimizer and a loss function. Note that there was no loss function used in  $\mathcal{M}_1$ . Finally, the training of the  $\mathcal{M}_2$  model is carried out successfully as all the loss values are converged to zero for both scenarios of both cases and the loss graphs are plotted in Fig. 10. the testing of the model is performed successfully on the 30 different tensors in each scenario for both cases as designated in Fig. 2. The evaluation of the results of training and testing the  $\mathcal{M}_2$  is explained in the next section.

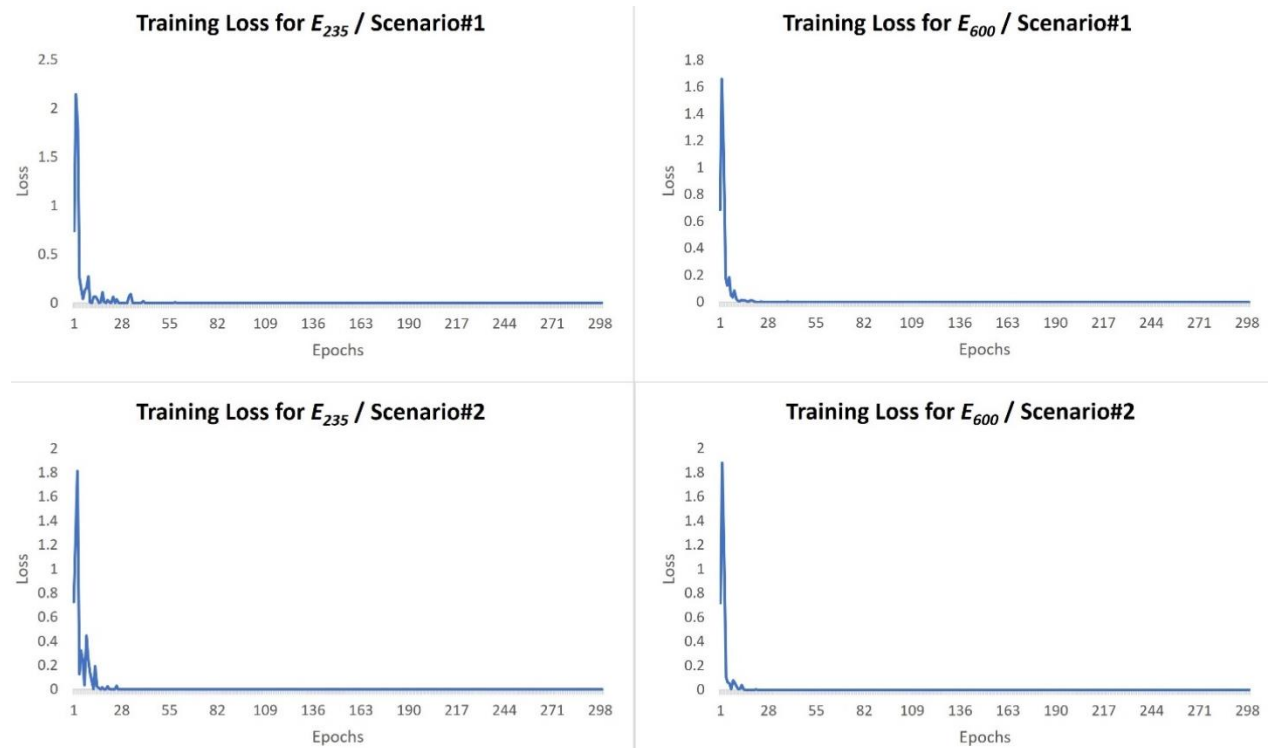


**Fig. 10.** Training plots of DCNN ( $\mathcal{M}_2$ ) of each scenario for case  $E_{235}$  and  $E_{600}$

## 2.8. $\mathcal{M}_2$ - Evaluation and Interpretation of Results

It is seen in the Fig. 10 that during the training of the  $\mathcal{M}_2$  model, the training loss functions are converged to zero in each scenario for both cases, in other words, the model learned the data effectively. Yet, the important part is in testing of the model, that is its performance on unseen data. For evaluating the results, one regression and one classification metrics are used. The classification metrics such as Classification Accuracy (CA) which is the ratio of total correct predictions over total predictions cannot be sufficient when an in-depth evaluation of performance of the model is needed. Since classification is converting the prediction score into a closest label

(0 or 1) based on the assumed threshold value, it might not reflect a good accuracy. For instance, a prediction score of 0.48 is converted into 0 (undamaged) if the assumed value of 0.49 as threshold is used for classification. This might not reflect the real performance of the model because that prediction score of 0.48 might be a result of 48% of damage (as a quantification of the damage such as 48% of bolt loosened) in the system or might be lot higher or lower and classifying it as label 0 can be a faulty prediction. An ROC and AUC curve can be employed to look for the optimum threshold value that gives the desired classification results for damage detection. Yet, this is not in the scope of this study and there are not many classification samples in the testing data; therefore, it is not necessary to check for all different thresholds. Thus, the threshold in this study is defined as 0.49 for the classification accuracy (CA). Moreover, it is possible for DL-based structural damage diagnostics that the probability of the tensor is undamaged or damaged can also mean the quantification result of the tensor whether it is undamaged or damaged. This is another area of investigation for different levels (detection, localization, quantification) of damage diagnostics using DL models. Along with a classification accuracy metric, a regression metric, Mean Absolute Error (MAE). MAE measures the average of all the prediction error by taking the summation of the absolute values of the predicted values minus the actual values, then dividing it by the total sample in the test. MAE is a great metric tool to measure the model's error on the dataset.

The resulted prediction scores along with the ground truths (correct target value) on the test tensors are bar plotted in Fig. 11 and Fig. 12 for cases  $E_{235}$  and  $E_{600}$  including each of their scenarios respectively. At first glance, it is easy to catch the close prediction scores to ground truths, particularly for the case  $E_{600}$  where the scores are closer since the  $\mathcal{M}_2$  is trained more. Likewise, the prediction scores are slightly closer to the ground truths in Scenario#1 in both cases since no synthetic tensor is involved in the process. Yet, more training helps the model to learn more about the data thus it can identify the test instances with more accuracy as this is the situation in both scenarios in case  $E_{600}$ . In Fig. 11, for the Scenario#1,  $\mathcal{M}_2$  is looking very consistent and confident on the test instances as it predicted all of them successfully. For the case  $E_{600}$ , Scenario#2, where the model is tested on only synthetic damaged and real undamaged instances have a slightly off prediction score around 0.10 on tensor 8, which might be negligible. Yet, the quantitative results can give better insight about the performance of the model. Hence, the results are reflected on the CA and MAE metrics, as in Fig. 13 and it is seen that the CAs are following the same scores, 100% and 97% for both cases and scenarios, respectively. Considering that even CA of 80% - 90% range is taken as success in most classification studies in DL field, the resulted CA values in this paper can be concluded as excellent. Lastly, the MAE results are seemingly very low which implies that  $\mathcal{M}_2$  has very low error values on the unseen data and the model can predict the damage associated instances from the undamaged data successfully.

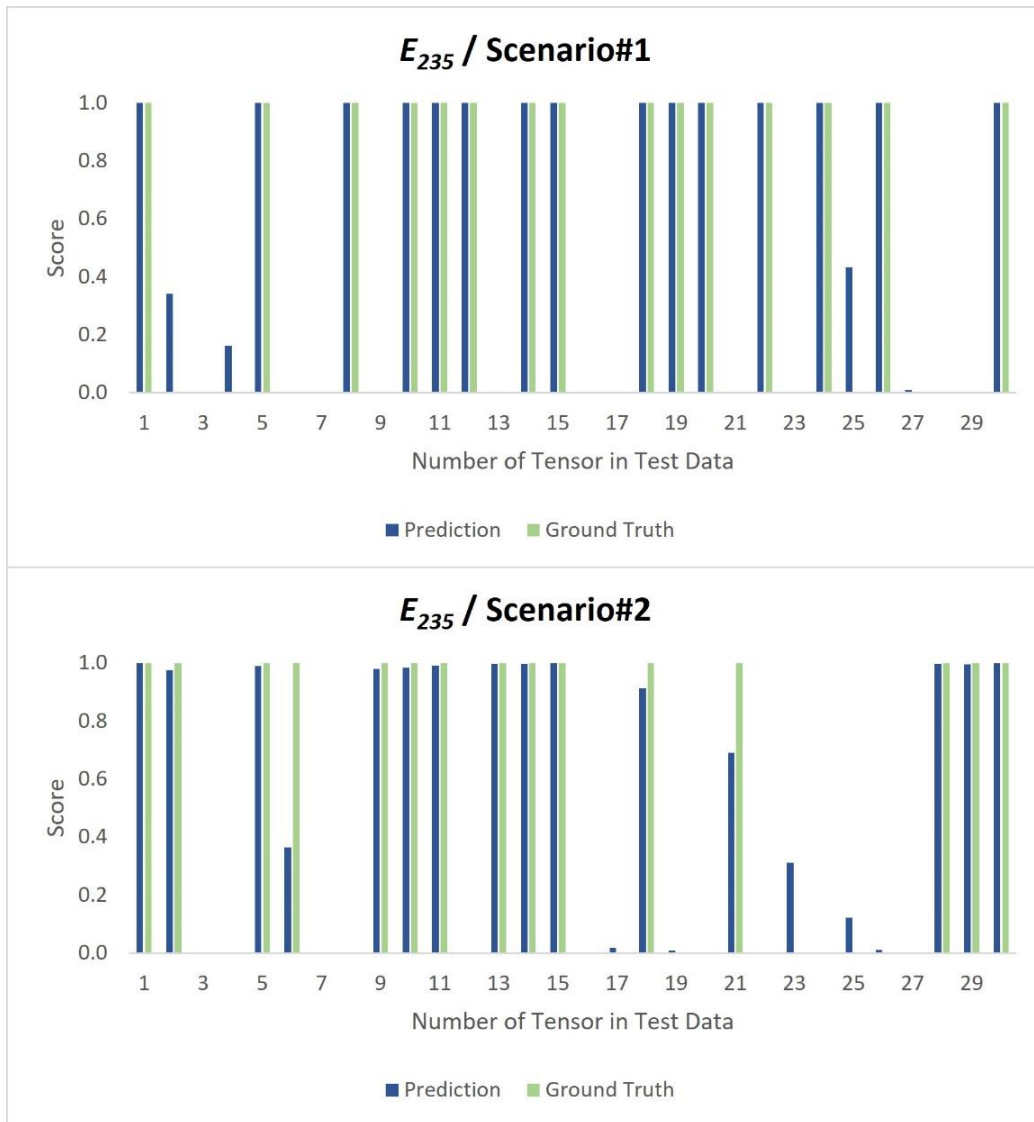


**Fig. 11.** Testing results of DCNN ( $\mathcal{M}_2$ ) for case  $E_{235}$

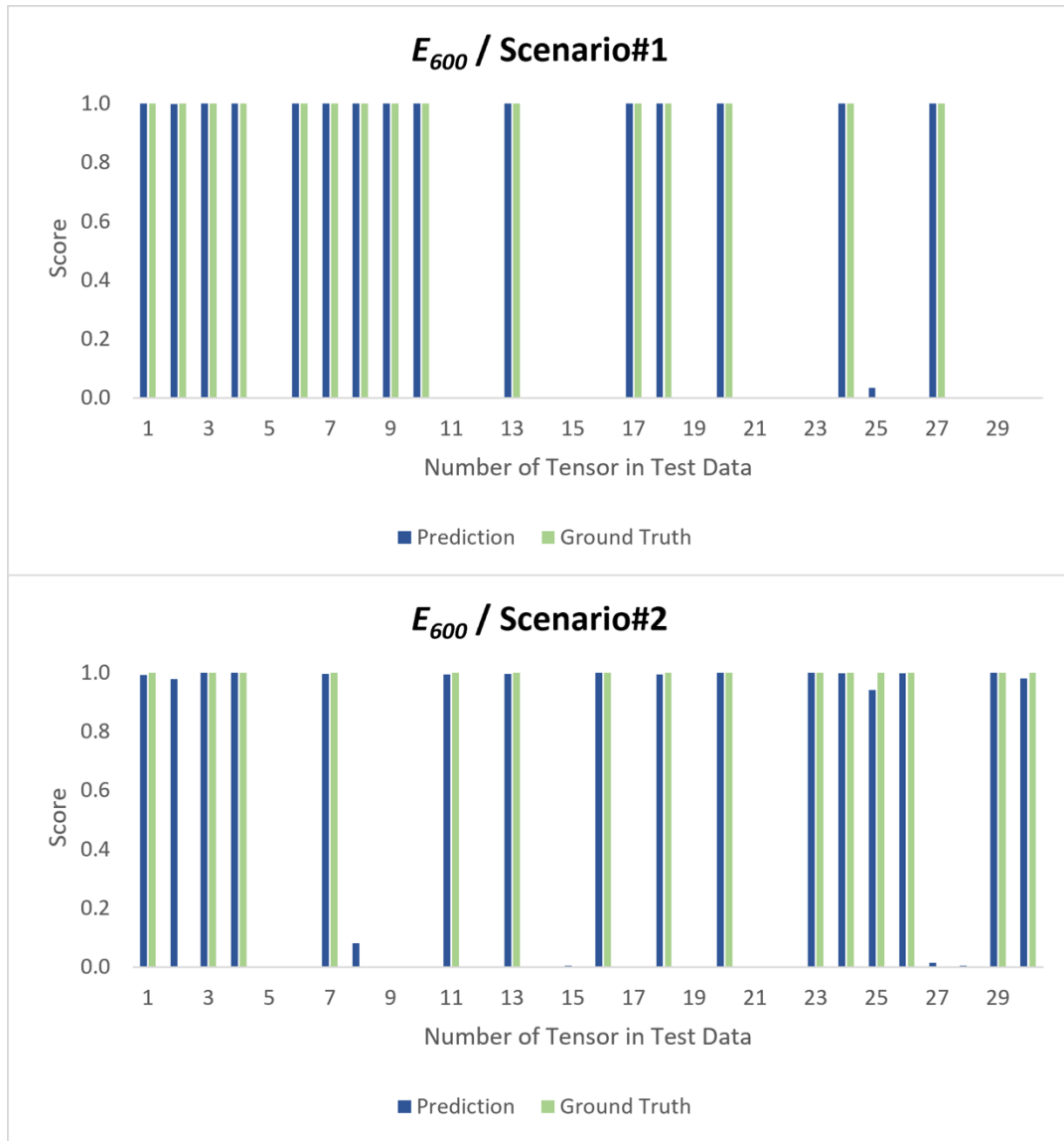


**Fig. 12.** Testing results of DCNN ( $\mathcal{M}_2$ ) for case  $E_{600}$

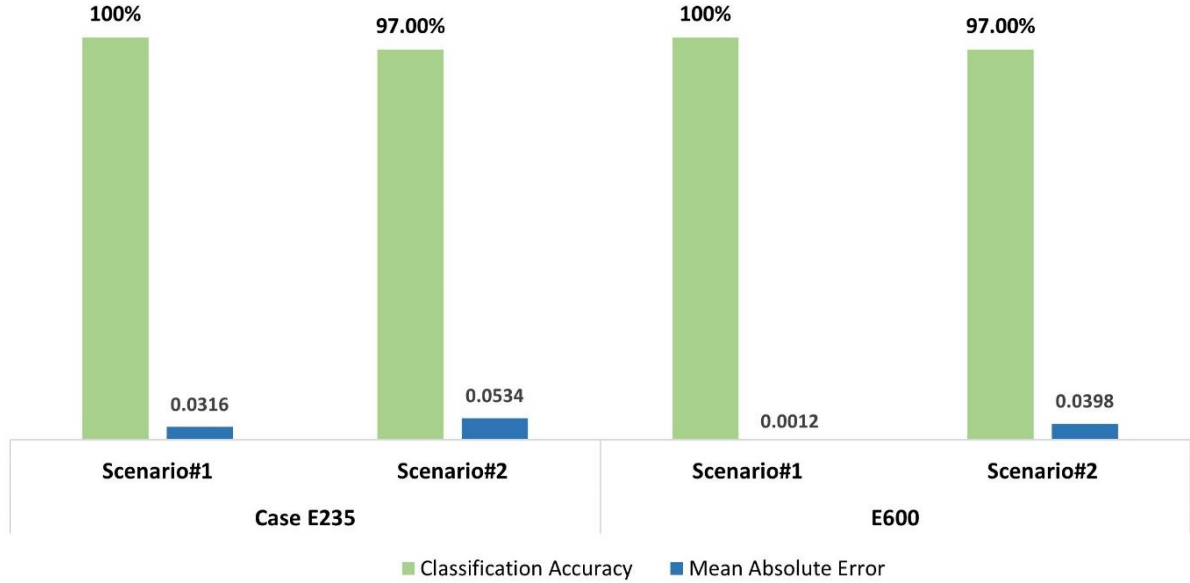


**Fig. 13.** Bar plot of Classification Accuracy and Mean Absolute Error of the testing results for case  $E_{235}$  and  $E_{600}$

### 3. Conclusions

Detecting and locating damage on large civil structures is a challenging task and has been subject of research for many years. Finding damage-associated vibration data from structures can also be very challenging. Therefore, data scarcity is a setback in civil SHM applications. With the rapid developments in the AI, ML, and DL, researchers started to take advantage of such tools for vibration-based structural damage diagnostics and achieved great success. Considering that the DL algorithms perform better with large data, this study used 1-D WGAN-GP for generating synthetic vibration data and validating the produced outputs by employing 1-D DCNN that is trained on real inputs and tested on synthetic dataset. For benchmarking purposes, the same DCNN model is also tested on real dataset. The classification results showed that the performance of DCNN on the test data is 97% and 100% on the real data with both scenarios resulting significantly low model errors. The main conclusions of this study can be listed in bullet points:

- The well-known problem of data scarcity in SHM of civil structures can be tackled by using GANs to generate similar types of datasets. This study showed that GANs can produce a vibration signal that is almost indistinguishable from the real ones and the generated signals are verified with metrics. Although this study used one of the most advanced GAN method, WGAN-GP algorithm, which improves the well-known training problems of GANs, the training is still tedious.
- The study demonstrated that the generated vibration signals are indistinguishable by DCNN. This means that in a situation where some damage-associated dataset exists for a civil structure, yet the amount of existed dataset is not sufficient for vibration-based damage diagnostics via DL model, then the proposed methodology can be used as a solution. As a result, the presented methodology paves the way for more ML and DL based models to be utilized for structural damage diagnostics.

- The generated data from GAN is creative and diversative enough that it is not a copy of the input nor a copy other generated datasets. The analogy is indeed similar to the real structures where dynamic responses for different damage types can contain similar characteristics in the raw data, yet they are not copies of each other. Therefore, when the data is scarce or portion of it is missing, GANs can be used to generate additional data that is similar “enough” to the original data. It also diversifies the input data by adding new meanings to the learned variation range of the dataset. Hence, it can be used successfully for vibration-based nonparametric damage diagnostics as demonstrated in this study.
- Based on the demonstrated performance herein by GANs on generating vibration data, there is good potential for further use of them in civil SHM applications. More research is needed to be able to generate the damaged dynamic response of structures using the undamaged responses.

### Data Availability Statement

Vibration data used in this study was made available in Abdeljaber et al., 2017. Some or all used models, codes, and detailed results are available from the corresponding author of this paper upon request.

### Acknowledgement

The authors would like to thank members of CITRS (Civil Infrastructure Technologies for Resilience and Safety) Research Initiative at the University of Central Florida. The second author would like to acknowledge the support by National Aeronautics and Space Administration (NASA) Award No. 80NSSC20K0326.

### Nomenclature

| Symbol        | Description   |
|---------------|---|
| $[a_{01}]_r$  | Vibration data at joint#1 in undamaged scenario (0) in raw form (262,144 samples)       |
| $[a_{11}]_r$  | Vibration data at joint#1 in damaged scenario (1) in raw form (262,144 samples)         |
| $[a_{11}]_b$  | Vibration tensor at joint#1 in damaged scenario (1) in batched form (1024 samples)      |
| $[a_{01}]_b$  | Vibration tensor at joint#1 in undamaged scenario (0) in batched form (1024 samples)    |
| $[a_{11f}]_b$ | Generated, “fake”, vibration tensor from GAN which the model is trained on $[a_{11}]_r$ |
| $E_{235}$     | Case where the GAN trained for 235 epochs   |

|                 |   |
|-----------------|---|
| $E_{600}$       | Case where the GAN trained for 600 epochs |
| $\mathcal{M}_1$ | Used 1-D WDCGAN-GP model in the paper     |
| $\mathcal{M}_2$ | Used 1-D DCNN model in the paper          |

## References

Abdeljaber, O. and Avci, O., Nonparametric Structural Damage Detection Algorithm for Ambient Vibration Response: Utilizing Artificial Neural Networks and Self-Organizing Maps, *Journal of Architectural Engineering*, vol. **22**, no. 2, June 2016. DOI: 10.1061/(ASCE)AE.1943-5568.0000205

Abdeljaber, O., Avci, O., Kiranyaz, M. S., Boashash, B., Sodano, H. and Inman, D. J., 1-D CNNs for Structural Damage Detection: Verification on a Structural Health Monitoring Benchmark Data, *Neurocomputing*, vol. **275**, January 2018. DOI: 10.1016/j.neucom.2017.09.069

Abdeljaber, O., Avci, O., Kiranyaz, S., Gabbouj, M. and Inman, D. J., Real-Time Vibration-Based Structural Damage Detection Using One-Dimensional Convolutional Neural Networks, *Journal of Sound and Vibration*, vol. **388**, February 2017. DOI: 10.1016/j.jsv.2016.10.043

Alom, M. Z., Taha, T. M., Yakopcic, C., Westberg, S., Sidike, P., Nasrin, M. S., Hasan, M., Essen, B. C. van, Awwal, A. A. S. and Asari, V. K., A State-of-the-Art Survey on Deep Learning Theory and Architectures, *Electronics*, vol. **8**, no. 3, March 5, 2019. DOI: 10.3390/electronics8030292

Arjovsky, M., Chintala, S. and Bottou, L., Wasserstein GAN, January 26, 2017.

Avci, O., Abdeljaber, O., Kiranyaz, S., Hussein, M., Gabbouj, M. and Inman, D. J., A Review of Vibration-Based Damage Detection in Civil Structures: From Traditional Methods to Machine Learning and Deep Learning Applications, *Mechanical Systems and Signal Processing*, vol. **147**, p. 107077, accessed October 12, 2021, January 15, 2021. DOI: 10.1016/J.YMSSP.2020.107077

Avci, O., Abdeljaber, O., Kiranyaz, S. and Inman, D., Structural Damage Detection in Real Time: Implementation of 1D Convolutional Neural Networks for SHM Applications, 2017.

Bandara, R. P., Chan, T. H. and Thambiratnam, D. P., Structural Damage Detection Method Using Frequency Response Functions, *Structural Health Monitoring*, vol. **13**, no. 4, July 19, 2014. DOI: 10.1177/1475921714522847

Borji, A., Pros and Cons of GAN Evaluation Measures, February 9, 2018.

Catbas, F. N. and Malekzadeh, M. (2016) "A Machine Learning Based Algorithm for Processing Massive (Big) Data Collected from the Mechanical Components of Movable Bridges" *Journal of Automation in Construction*, Elsevier, Vol 72, Part3, December 2016, Pages 269–278



- Catbas, F.N., Hiasa, S., Dong, C, Pan,Y., Celik, O. and Karaaslan, E. (2017) “Comprehensive structural health monitoring at local and global level with vision-based technologies”, *26th ASTN symposium*, 10-21, Jacksonville, FL, Mar.13 -16, 2017
- Catbas, F.N., Brown, D.L., and Aktan, A.E. (2006) “Use of Modal Flexibility for Damage Detection and Condition Assessment: Case Studies and Demonstrations on Large Structures,” *Journal of Structural Engineering*, ASCE, Vol.132, No 11, pp.1699-1712.
- Catbas, F.N. and Aktan, A.E. (2002) "Condition and Damage Assessment: Issues and Some Promising Indices", *Journal of Structural Engineering*, ASCE, Vol.128, No. 8, pp.1026-1036.
- Costa, V., Lourenço, N., Correia, J., and Machado, P., COEGAN, *Proceedings of the Genetic and Evolutionary Computation Conference*, New York, NY, USA: ACM, 2019.
- Cury, A. and Crémona, C., Pattern Recognition of Structural Behaviors Based on Learning Algorithms and Symbolic Data Concepts, *Structural Control and Health Monitoring*, vol. **19**, no. 2, March 2012. DOI: 10.1002/stc.412
- Das, S., Saha, P. and Patro, S. K., Vibration-Based Damage Detection Techniques Used for Health Monitoring of Structures: A Review, *Journal of Civil Structural Health Monitoring*, vol. **6**, no. 3, July 9, 2016. DOI: 10.1007/s13349-016-0168-5
- Dong, C.-Z. and Catbas, F. N., A Review of Computer Vision–Based Structural Health Monitoring at Local and Global Levels, *Structural Health Monitoring*, vol. **20**, no. 2, March 20, 2021. DOI: 10.1177/1475921720935585
- Eren, L., Bearing Fault Detection by One-Dimensional Convolutional Neural Networks, *Mathematical Problems in Engineering*, vol. **2017**, 2017. DOI: 10.1155/2017/8617315
- Fan, G., Li, J., Hao, H. and Xin, Y., Data Driven Structural Dynamic Response Reconstruction Using Segment Based Generative Adversarial Networks, *Engineering Structures*, vol. **234**, May 2021. DOI: 10.1016/j.engstruct.2021.111970
- Gao, S., Wang, X., Miao, X., Su, C. and Li, Y., ASM1D-GAN: An Intelligent Fault Diagnosis Method Based on Assembled 1D Convolutional Neural Network and Generative Adversarial Networks, *Journal of Signal Processing Systems*, vol. **91**, no. 10, October 3, 2019. DOI: 10.1007/s11265-019-01463-8
- GARDNER, P., and BARTHORPE, R. J., On Current Trends in Forward Model-Driven SHM, *Structural Health Monitoring 2019*, Lancaster, PA: DEStech Publications, Inc., 2019.
- Ghiasi, R., Torkzadeh, P. and Noori, M., A Machine-Learning Approach for Structural Damage Detection Using Least Square Support Vector Machine Based on a New Combinational Kernel Function, *Structural Health Monitoring*, vol. **15**, no. 3, May 11, 2016. DOI: 10.1177/1475921716639587

González, M. P. and Zapico, J. L., Seismic Damage Identification in Buildings Using Neural Networks and Modal Data, *Computers & Structures*, vol. **86**, no. 3–5, February 2008. DOI: 10.1016/j.compstruc.2007.02.021

Goodfellow, I., NIPS 2016 Tutorial: Generative Adversarial Networks, December 31, 2016.

Goodfellow, I. J., Pouget-Abadie, J., Mirza, M., Xu, B., Warde-Farley, D., Ozair, S., Courville, A. and Bengio, Y., Generative Adversarial Networks, June 10, 2014.

Guan, S. and Loew, M., A Novel Measure to Evaluate Generative Adversarial Networks Based on Direct Analysis of Generated Images, February 27, 2020.

Gul, M. and Catbas, F. N., Ambient Vibration Data Analysis for Structural Identification and Global Condition Assessment, *Journal of Engineering Mechanics*, vol. **134**, no. 8, August 2008. DOI: 10.1061/(ASCE)0733-9399(2008)134:8(650)

Gul, M. and Catbas, F. N., Damage Assessment with Ambient Vibration Data Using a Novel Time Series Analysis Methodology, *Journal of Structural Engineering*, vol. **137**, no. 12, December 2011. DOI: 10.1061/(ASCE)ST.1943-541X.0000366

Gul, M., Dumlupinar, T., Hattori, H. and Catbas, F. N. “Structural monitoring of movable bridge mechanical components for maintenance decision-making”, *Structural Monitoring and Maintenance Journal*, Vol. 1, No. 3, 2014, pp. 249-271

Gulrajani, I., Ahmed, F., Arjovsky, M., Dumoulin, V. and Courville, A., Improved Training of Wasserstein GANs, March 31, 2017.

Guo, Q., Li, Y., Song, Y., Wang, D. and Chen, W., Intelligent Fault Diagnosis Method Based on Full 1-D Convolutional Generative Adversarial Network, *IEEE Transactions on Industrial Informatics*, vol. **16**, no. 3, March 2020. DOI: 10.1109/TII.2019.2934901

Heusel, M., Ramsauer, H., Unterthiner, T., Nessler, B. and Hochreiter, S., GANs Trained by a Two Time-Scale Update Rule Converge to a Local Nash Equilibrium, June 26, 2017.

Jiang, H., Wan, C., Yang, K., Ding, Y. and Xue, S., Continuous Missing Data Imputation with Incomplete Dataset by Generative Adversarial Networks–Based Unsupervised Learning for Long-Term Bridge Health Monitoring, *Structural Health Monitoring*, June 4, 2021. DOI: 10.1177/14759217211021942

Krishnan Nair, K. and Kiremidjian, A. S., Time Series Based Structural Damage Detection Algorithm Using Gaussian Mixtures Modeling, *Journal of Dynamic Systems, Measurement, and Control*, vol. **129**, no. 3, May 1, 2007. DOI: 10.1115/1.2718241

Kuo, P.-H., Lin, S.-T. and Hu, J., DNAE-GAN: Noise-Free Acoustic Signal Generator by Integrating Autoencoder and Generative Adversarial Network, *International Journal of Distributed Sensor Networks*, vol. **16**, no. 5, May 20, 2020. DOI: 10.1177/1550147720923529

- Lee, J. J., Lee, J. W., Yi, J. H., Yun, C. B. and Jung, H. Y., Neural Networks-Based Damage Detection for Bridges Considering Errors in Baseline Finite Element Models, *Journal of Sound and Vibration*, vol. **280**, no. 3–5, February 2005. DOI: 10.1016/j.jsv.2004.01.003
- Lee, J. and Kim, S., Structural Damage Detection in the Frequency Domain Using Neural Networks, *Journal of Intelligent Material Systems and Structures*, vol. **18**, no. 8, August 29, 2007. DOI: 10.1177/1045389X06073640
- Luo, T., Fan, Y., Chen, L., Guo, G. and Zhou, C., EEG Signal Reconstruction Using a Generative Adversarial Network with Wasserstein Distance and Temporal-Spatial-Frequency Loss, *Frontiers in Neuroinformatics*, vol. **14**, April 30, 2020. DOI: 10.3389/fninf.2020.00015
- Pathirage, C. S. N., Li, J., Li, L., Hao, H., Liu, W. and Ni, P., Structural Damage Identification Based on Autoencoder Neural Networks and Deep Learning, *Engineering Structures*, vol. **172**, October 2018. DOI: 10.1016/j.engstruct.2018.05.109
- Radford, A., Metz, L. and Chintala, S., Unsupervised Representation Learning with Deep Convolutional Generative Adversarial Networks, November 19, 2015.
- Rastin, Z., Ghodrati Amiri, G. and Darvishan, E., Unsupervised Structural Damage Detection Technique Based on a Deep Convolutional Autoencoder, *Shock and Vibration*, vol. **2021**, April 23, 2021. DOI: 10.1155/2021/6658575
- Sabir, R., Rosato, D., Hartmann, S., and Guhmann, C., Signal Generation Using 1d Deep Convolutional Generative Adversarial Networks for Fault Diagnosis of Electrical Machines, *2020 25th International Conference on Pattern Recognition (ICPR)*, IEEE, 2021.
- Salimans, T., Goodfellow, I., Zaremba, W., Cheung, V., Radford, A. and Chen, X., Improved Techniques for Training GANs, June 10, 2016.
- Santos, A., Figueiredo, E., Silva, M. F. M., Sales, C. S. and Costa, J. C. W. A., Machine Learning Algorithms for Damage Detection: Kernel-Based Approaches, *Journal of Sound and Vibration*, vol. **363**, February 2016. DOI: 10.1016/j.jsv.2015.11.008
- Shang, Z., Sun, L., Xia, Y. and Zhang, W., Vibration-Based Damage Detection for Bridges by Deep Convolutional Denoising Autoencoder, *Structural Health Monitoring*, vol. **20**, no. 4, July 28, 2021. DOI: 10.1177/1475921720942836
- Shao, S., Wang, P. and Yan, R., Generative Adversarial Networks for Data Augmentation in Machine Fault Diagnosis, *Computers in Industry*, vol. **106**, April 2019. DOI: 10.1016/j.compind.2019.01.001
- Silva, M., Santos, A., Figueiredo, E., Santos, R., Sales, C. and Costa, J. C. W. A., A Novel Unsupervised Approach Based on a Genetic Algorithm for Structural Damage Detection in Bridges, *Engineering Applications of Artificial Intelligence*, vol. **52**, June 2016. DOI: 10.1016/j.engappai.2016.03.002

Truong, T., and Yanushkevich, S., Generative Adversarial Network for Radar Signal Synthesis, *2019 International Joint Conference on Neural Networks (IJCNN)*, IEEE, 2019.

Wang, T., Trugman, D. and Lin, Y., SeismoGen: Seismic Waveform Synthesis Using GAN With Application to Seismic Data Augmentation, *Journal of Geophysical Research: Solid Earth*, vol. **126**, no. 4, April 16, 2021. DOI: 10.1029/2020JB020077

Wang, Z., Bovik, A. C., Sheikh, H. R. and Simoncelli, E. P., Image Quality Assessment: From Error Visibility to Structural Similarity, *IEEE Transactions on Image Processing*, vol. **13**, no. 4, April 2004. DOI: 10.1109/TIP.2003.819861

Wulan, N., Wang, W., Sun, P., Wang, K., Xia, Y. and Zhang, H., Generating Electrocardiogram Signals by Deep Learning, *Neurocomputing*, vol. **404**, September 2020. DOI: 10.1016/j.neucom.2020.04.076

Yin, T., Lam, H. F., Chow, H. M. and Zhu, H. P., Dynamic Reduction-Based Structural Damage Detection of Transmission Tower Utilizing Ambient Vibration Data, *Engineering Structures*, vol. **31**, no. 9, September 2009. DOI: 10.1016/j.engstruct.2009.03.004

Yu, Y., Wang, C., Gu, X. and Li, J., A Novel Deep Learning-Based Method for Damage Identification of Smart Building Structures, *Structural Health Monitoring*, vol. **18**, no. 1, January 8, 2019. DOI: 10.1177/1475921718804132

Zhang, C., Kuppannagari, S. R., Kannan, R., and Prasanna, V. K., Generative Adversarial Network for Synthetic Time Series Data Generation in Smart Grids, *2018 IEEE International Conference on Communications, Control, and Computing Technologies for Smart Grids (SmartGridComm)*, IEEE, 2018.

Zhang, X., Qin, Y., Yuen, C., Jayasinghe, L. and Liu, X., Time-Series Regeneration with Convolutional Recurrent Generative Adversarial Network for Remaining Useful Life Estimation, January 10, 2021.